

Supplemental methods

Patients. Children with FCD type II (n=10, age range: 1-16 years) who underwent epilepsy surgery were recruited at the Fondation Rothschild (Paris, France) in 2016-2017 for the study.

Deep sequencing. Genomic DNA was extracted from peripheral blood lymphocytes and from flash-frozen resected brain tissue of FCD participants using Maxwell DNA purification kit (Promega). We used a custom gene panel of 25 genes belonging to the GATOR1/mTOR and PI3K/AKT/mTOR pathways previously published (7). Deep targeted capture sequencing (1820X mean coverage; 99.9% of bases with coverage >100X) and detection of the low frequency (<10%) somatic variants with samtools-1.1 (mpileup) were previously reported (7). Variants were confirmed using alternative sequencing technologies to exclude sequencing artifacts: conventional Sanger sequencing and ultra-deep site-specific amplicon sequencing of a 250bp PCR-amplified fragment encompassing both *DEPDC5* variants on a MiSeq (212,000X mean coverage).

Neuropathology and immunostaining. Histopathological diagnosis was made according to the classification of the International League Against Epilepsy (ILAE) Diagnostic Methods Commission (8). Formalin-fixed paraffin-embedded (FFPE) sections (6µm) of resected brain specimen were used for immunostaining using standard procedures. mTORC1 activity was assessed by visualizing the phosphorylation levels of one of its downstream effector, the ribosomal protein S6. Brain sections were probed overnight at 4°C with antibody against Ser240/244 phosphorylated S6 (Cell Signaling #5364, Lot 0006, 1:400) and NeuN (Millipore #MAB377, Clone A60, Lot 2639366), then probed for 1h at room-temperature using appropriate AlexaFluor488/555-conjugated secondary antibodies (ThermoFisher #A28175, #A32732).

Selection of CRISPR-Cas9 gRNAs. To introduce CRISPR-Cas9 mediated mosaic deleterious indels into mouse *Depdc5*, we used ChopChop webtool (<http://chopchop.cbu.uib.no>) to select guide RNAs (gRNA) ranked according to their highest in silico predicted efficiency and lowest off-target (no off-target considering 3 mismatches) on the mm10/GRCm38 mouse genome (*Depdc5* transcript NM_001025426). Out of the top 6 gRNAs,

we selected 2 gRNAs targeting *Depdc5* on the most 5' coding region of the gene, both located on exon 16 (chr5:32903876 and chr5:32903826), for which the cleavage efficiency was predicted in silico at 71 and 75%.

DNA constructs. The pX330 plasmid was purchased from AddGene (#42230) and modified by inserting a PCR-amplified T2A-mRuby2 sequence following Gibson Assembly (NEB #E2611L) at the EcoRI restriction site according to manufacturer recommendations. The plasmids containing T2A-mRuby2 and the pCAG-EGFP were kindly provided by Benoit Bruneau (Gladstone Institutes, UCSF). The pCAG-EGxxFP plasmid was purchased from AddGene (#50716) and modified by cloning exon 16 target-containing PCR-amplified fragment by Gibson Assembly (NEB) between the BamHI and Sall restriction sites. Plasmid DNAs were amplified and purified with the Nucleobond Xtra Maxi EF kit (Macherey-Nagel). All insert vectors were Sanger sequenced.

Cell culture and transfection. HEK293T cells (ATCC #CRL-1573) were grown in DMEM (ThermoFisher #61965026) supplemented with 10% FBS (ThermoFisher #10270106) at 37°C and 5% CO₂. Restorable EGFP strategy for the validation of CRISPR-Cas9 constructs efficiency was performed as described (30). Transfection was performed with Lipofectamine 2000 (ThermoFisher #11668019) following manufacturer's recommendation. Three independent transfection experiments were done. For each experiment, five fields per condition were imaged at 20x using an EVOS FL inverted microscope (ThermoFisher #AMEFC4300). mRuby2⁺ and GFP⁺ cells were manually counted on ImageJ.

In utero electroporation. All experiments were performed in the same time, in the morning and we worked with Swiss-Webster mice (Janvier labs), an outbred strain which is not prone to epileptic activity. Embryos at E14.5 from pregnant Swiss-Webster mice were injected with both EGFP and CRISPR-Cas9 plasmids in the right lateral ventricle. IUE were performed in the same time in the morning to improve reproducibility. Mice were injected with buprenorphine 30min before surgery, anesthetized initially with 4% isoflurane and maintained under 2% oxygen/isoflurane mix during the procedure. Uterine horns were exposed and a solution

containing 2.5mg/mL of CRISPR-Cas9 or 2.5mg/mL of pX330-empty and 0.5mg/mL of pCAG-EGFP mixed with 10% FastGreen (1mg/mL) was injected into the lateral ventricle of embryos. Electrodes were placed around the skull to target the dorso-medial part of the cortex and electric pulses using a NEPA21 super electroporator (NepaGene) were delivered as follows: 3 poring pulses of 40V for 30ms with intervals of 450ms and decay rate of 10% followed by 5 transfer pulses of 25V for 50ms with intervals of 450ms and decay rate of 40%. Only embryos or newborn pups expressing GFP were selected for further experiments (both males and females). All efforts were made to minimize the suffering and number of animals used.

Preparation of brain slices. Embryonic brains were collected in the morning at E18.5 and placed into PBS 0.1M + 4% paraformaldehyde (PFA) at 4°C overnight prior to transfer into PBS. 80µm coronal sections were cut using a vibratome. Adult animals were perfused with PBS 0.1M + 0.9% sodium chloride/heparin followed by PBS 0.1M + 4% PFA prior to transfer into PBS 0.1M + 4% PFA at 4°C for 48h and PBS 0.1M + 30% sucrose (w/vol) solution. Brains of mice who died from seizures were collected and placed in PBS 0.1M + 4% PFA at 4°C for 48h prior to transfer in PBS 0.1M + 30% sucrose (w/vol) solution. 20µm coronal sections were prepared using a cryostat.

Migration analysis. Boundaries of each layer for SVZ, IZ and CP were determined using DAPI images of 80µm coronal sections from E18.5 embryos. Corresponding GFP images were converted into binary files and processed with ImageJ watershed. Regions of interest were cropped and processed with ImageJ analyze particles to count the number of cell soma. Raw numbers of GFP+ cells per layer was normalized to the total number of counted GFP+ cells per ROI to determine the overall percentage of cell soma in each layer for each slice. For adult animals, cortical layer boundaries were determined using DAPI and NeuroTrace-positive cell density on 20µm coronal sections of animals aged P21-P59. Regions of interest were cropped and GFP+ cells from different cortical layers were manually counted on ImageJ.

Fluorescence-Activated Cell Sorting (FACS). Embryos were collected at E18.5. GFP+ brain hemispheres were isolated and dissociated to single cell suspension with 0.05% trypsin/EDTA. Between 30.000 and 100.000 living GFP+ cells, identified as impermeable to propidium iodide,

were FACS-sorted with a BD FACSAria II. Gating for GFP+ cells was determined on single-cell suspension from brains of non-electroporated animals and reported on single-cell suspension from brain hemispheres of control and *Depdc5*^{fKO-gRNA1}. Genomic DNA was extracted using the NucleoSpin Tissue XS kit (Macherey Nagel #740901). Ultra-deep site-specific amplicon sequencing was performed as in sequencing methods section. Primers for the 250bp amplicon were designed to encompass the Cas9 cleaving site.

Immunostaining. 20µm mounted brain slices were probed overnight at 4°C with primary antibody anti-pS6 ribosomal protein (Ser240/244; Cell Signaling #5364, Lot 0006, 1:400), then probed for 1h at room-temperature with secondary antibody AlexaFluor555-conjugated goat anti-rabbit (1:1000; ThermoFisher #A32732). NeuroTrace Red Fluorescent Nissl Stain was performed following manufacturer's recommendations (ThermoFisher #N21482). Hematoxylin-eosin staining was performed using standard techniques.

Cell size and mTORC1 activity. We measured soma area and pS6 mean intensity of all GFP+ brain cells present on the considered coronal slice. We then randomly selected equivalent numbers of contralateral GFP-negative cells and ipsilateral GFP+ cells over DAPI staining of nuclei and measured their soma size and pS6 intensities. We detected 24-70 GFP+ cells per slice. Fold change in soma area and pS6 levels were calculated by dividing values from each ipsilateral GFP+ cell by the mean of the values from contralateral GFP-negative cells. Animals were aged between P50 and P60, or were younger if they experienced lethal seizure (P37, P41, P54).

Rapamycin administration. 8h after in utero electroporation, pregnant females were injected intraperitoneally, in the right lower quadrant of the abdomen to avoid damaging uterine horns and embryos, with a dose of 1mg/kg of rapamycin (LC-Laboratories #R-5000). Solution was prepared freshly from a stock solution of 40mg/mL in 100% ethanol of rapamycin diluted in a stock vehicle solution of PBS 0.1M + 5% polyethylene glycol 300 + 5% Tween 20, to a final concentration of 4% ethanol (v/v).

Animal surgery and intracranial electrode implantation. Mice aged P19-P25 (n=13 *Depdc5*^{fKO-1}, n=8 controls injected with Cas9 constructs without gRNA) were anesthetized with

4 to 2% isoflurane 30min following analgesic administration (0.1mg/kg buprenorphine) and placed in a stereotaxic frame. Enamel-coated stainless-steel electrodes were implanted on the left and right primary motor cortex (M1: AP, 2.2 mm; MD, 2.2 mm), on the left lateral parietal association cortex (LPta: AP, -1.8 mm; MD, -1.2 mm), and a common reference in the cerebellum. A bipolar electrode was inserted into the right hippocampus (A-P, -1.8 mm; MD, -1.2 mm; 1.7 mm below the cortical surface), as previously described (14). All coordinates were derived and adjusted from the Paxinos and Watson mice brain atlas.

EEG recordings. After a recovery period, mice were placed under freely moving conditions and connected to an ADC amplifier (Brainbox EEG-1166), part of an EEG-Video acquisition system (Deltamed, Natus). EEG signals were acquired at 2048Hz and band pass filtered between 0.5 and 70Hz. The video was synchronized to the electrophysiological signal and recorded at 25 frames/s. *Depdc5^{fKO}* animals (n=13) were continuously recorded from P21 until P91 (or until lethal seizure occurred) for at least three consecutive days/week (24/24h) and control animals with Cas9-expressing constructs without gRNA (n=8) were continuously recorded from P30 to P60 for at least two consecutive days/week. Analysis of EEG recordings was manually performed by two independent experimenters (one blind to the genotype). Visual seizure detection was based on pattern criteria used for human epileptic patients. Each channel and animal was analyzed independently over a sliding window corresponding to 20s. Signal and Fast Fourier Transform (FFT) analyses were achieved using Gabor function running in MATLAB (Mathworks, USA). Morlet wavelets were computed in the 1-50 Hz frequency.

In vitro slice electrophysiology. Acute coronal brain slices (350 μ m) were obtained from P20-P24 *Depdc5^{fKO}* and control mice (only males). Animals were deeply anesthetized with isoflurane and decapitated. Brains were quickly removed and immersed in ice-cold (4°C) cutting solution containing (in mM): 230 sucrose, 26 NaHCO₃, 2.5 KCl, 1.25 NaH₂PO₄, 7 MgSO₄, 0.5 CaCl₂, 3 pyruvic acid, 3 myo-inositol, 0.4 ascorbic acid and 16 glucose, saturated with 95% O₂ / 5% CO₂. Slices were cut with a vibratome in cutting solution and incubated in oxygenated artificial cerebrospinal fluid (aSCF) containing (in mM): 126 NaCl, 2.5 KCl, 2 CaCl₂,

1 MgSO₄, 1.25 NaH₂PO₄, 26 NaHCO₃ and 20 glucose (pH 7.4), initially at 34°C for 30min, and subsequently at room temperature for at least another 30min, before being transferred to the recording chamber at 30°C. To compare neurons from the same cortical layer, recordings were obtained from layer III GFP+ pyramidal neurons of the somatosensory cortex. The most enlarged cells were too fragile to be patched. Glass electrodes (tip resistance of 2-4 MΩ) were filled with the following solution (in mM): 110 K-gluconate, 10 KCl, 10 HEPES, 1 EGTA, 4 Mg-ATP, 0.3 Na-GTP, 10 Na-phosphocreatine, 0.3% biocytine; pH adjusted to 7.2 with KOH; 280-300 mOsm. Whole-cell patch-clamp recordings were performed with a Multiclamp 700B amplifier (Molecular devices) and data were acquired with pClamp software (Molecular devices); signals were sampled at 20 and 50 kHz and filtered at 2 and 10 kHz for voltage and current-clamp mode, respectively. No junction potential correction was applied. Access resistance was typically <20 MΩ and carefully monitored; data were excluded if changes exceeded 20% during the recorded period. Spontaneous AMPA receptor-mediated excitatory synaptic events were pharmacologically isolated in the presence of 50μm picrotoxin (HelloBio #HB0506) and 50μm D-(-)-2-Amino-5-phosphonopentanoic acid (D-AP5, HelloBio #HB0225) in the aCSF bath perfusion to block inhibitory GABA_A receptors-mediated and glutamatergic NMDA receptor-mediated synaptic events, and recorded in voltage-clamp mode at a holding potential of -70 mV. During current clamp recordings, slices were continuously perfused with aCSF containing 20μm 6,7-Dinitroquinoxaline-2,3-dione (DNQX, Hello Bio #HB0262), an AMPA/kainate antagonist in addition to picrotoxin and D-AP5 to block fast inhibitory and excitatory synaptic transmission.

Electrophysiology data analysis. Resting membrane potential was determined at least 3-5 min after whole-cell recordings were established. Access resistance and membrane capacitance were calculated from the average current response to 50ms voltage steps of -5 mV repeated 50 times. Input resistance (R_{in}) and firing properties were determined in response to successive long current steps (1 s; -300 to +750 pA steps) with a 50pA increment while holding the cell at -70 mV. R_{in} was calculated as the slope of the current-voltage relationship between -70 to -65 mV. To determine the spike firing response, action potentials were detected

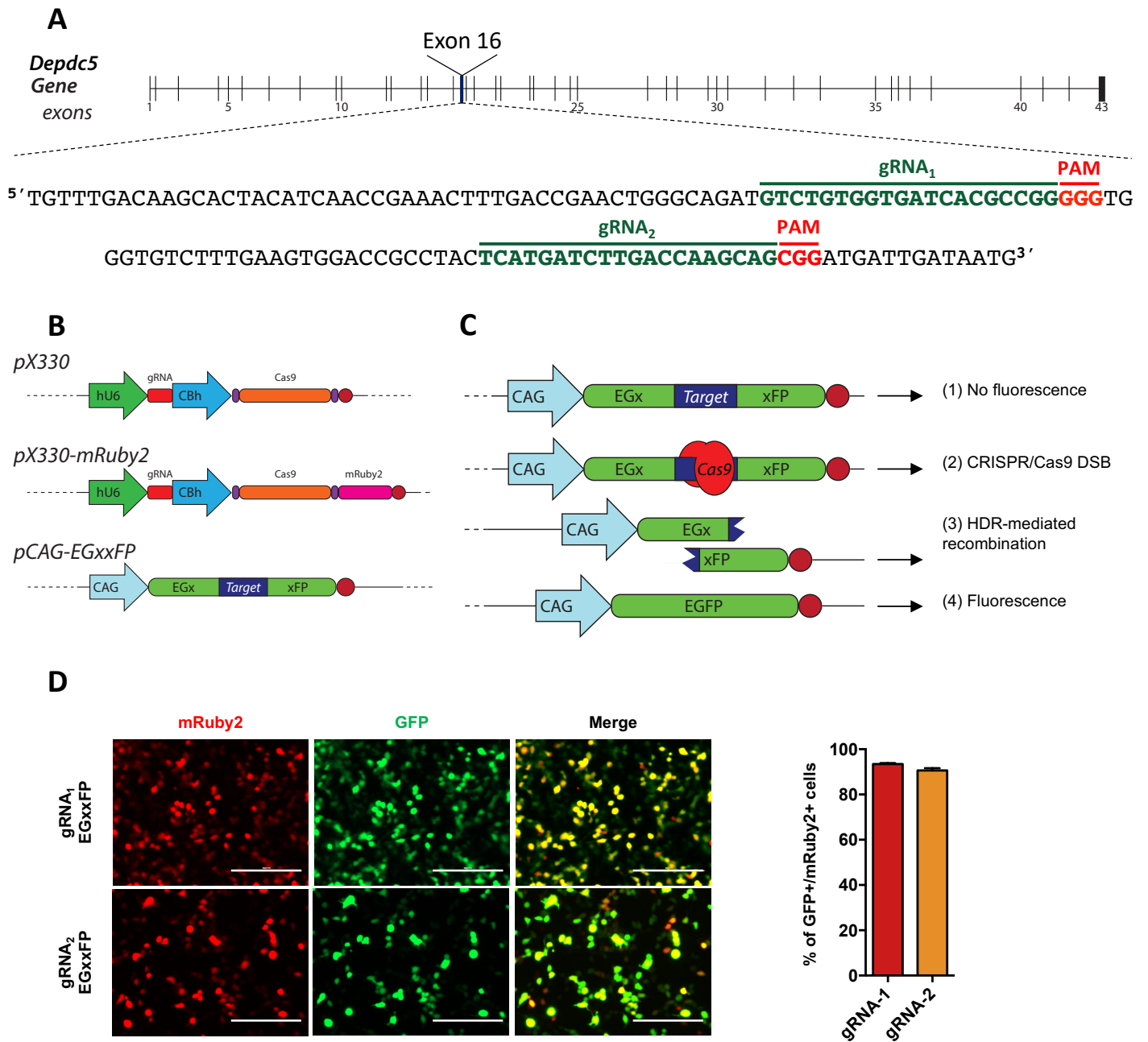
using a threshold criterion and the mean firing frequency was calculated (number of action potentials/s) for each step and plotted as an input-output relationship. The gain of the firing frequency was defined by the slope of a least-square linear regression performed on the fitted values predicted by the sigmoid fit over a frequency range of 25-75% of the maximal frequency. Passive and firing properties were analyzed with pClamp10 (Molecular devices), Prism7 (GraphPad) softwares and custom-written scripts (MATLAB, MathWorks). Synaptic currents were analysed using a custom-written software and OriginPro 2017 (OriginLab corporation).

Neuronal reconstruction. 350 μ m brain slices of mice aged P20-24 with biocytin-filled cells were fixed in PBS 0.1M + 4% PFA at 4°C overnight immediately following patch-clamp experiments. Slices were then incubated in PBS 0.1M + 0.4% Triton X-100 + 10% BSA for 3h and incubated with AlexaFluor 647-conjugated streptavidin antibody (ThermoFisher #S21374) in PBS 0.1M + 0.08% Triton X-100 + 2% BSA for 3h. Images were acquired on a Leica SP8 inverted confocal microscope with an oil-immersion HC PL APO 64x/1.40 objective at 2.05x zoom. Morphological neuronal reconstruction was performed with the neurofilament module of Imaris software. Length of dendrite segments was measured within concentric shells (Sholl analysis). Apical dendritic tuft width was defined as the distance between the two widest points of the tuft. Dendritic spines were manually analyzed on ImageJ over the dendritic shaft of the main basal dendrite and the apical dendrite.

Statistics. All data are presented as mean \pm SEM. All statistical analyses were performed in Prism 7 (GraphPad Software). All statistical analyses were two-tailed. Unmatched non-parametric (One-way and 2way) ANOVA were corrected with Tukey's post-test for multiple comparisons in Figure 2. Unmatched non-parametric 2way ANOVA for group effect was performed for Sholl analysis and mean firing frequency analysis. Unpaired t-test was performed for analysis of spine head width. Unpaired Mann-Whitney tests were performed without post-hoc corrections for electrophysiology analyses. *P* values lower than 0.05 were considered statistically significant. Exact *P* values were given when possible (*P*=).

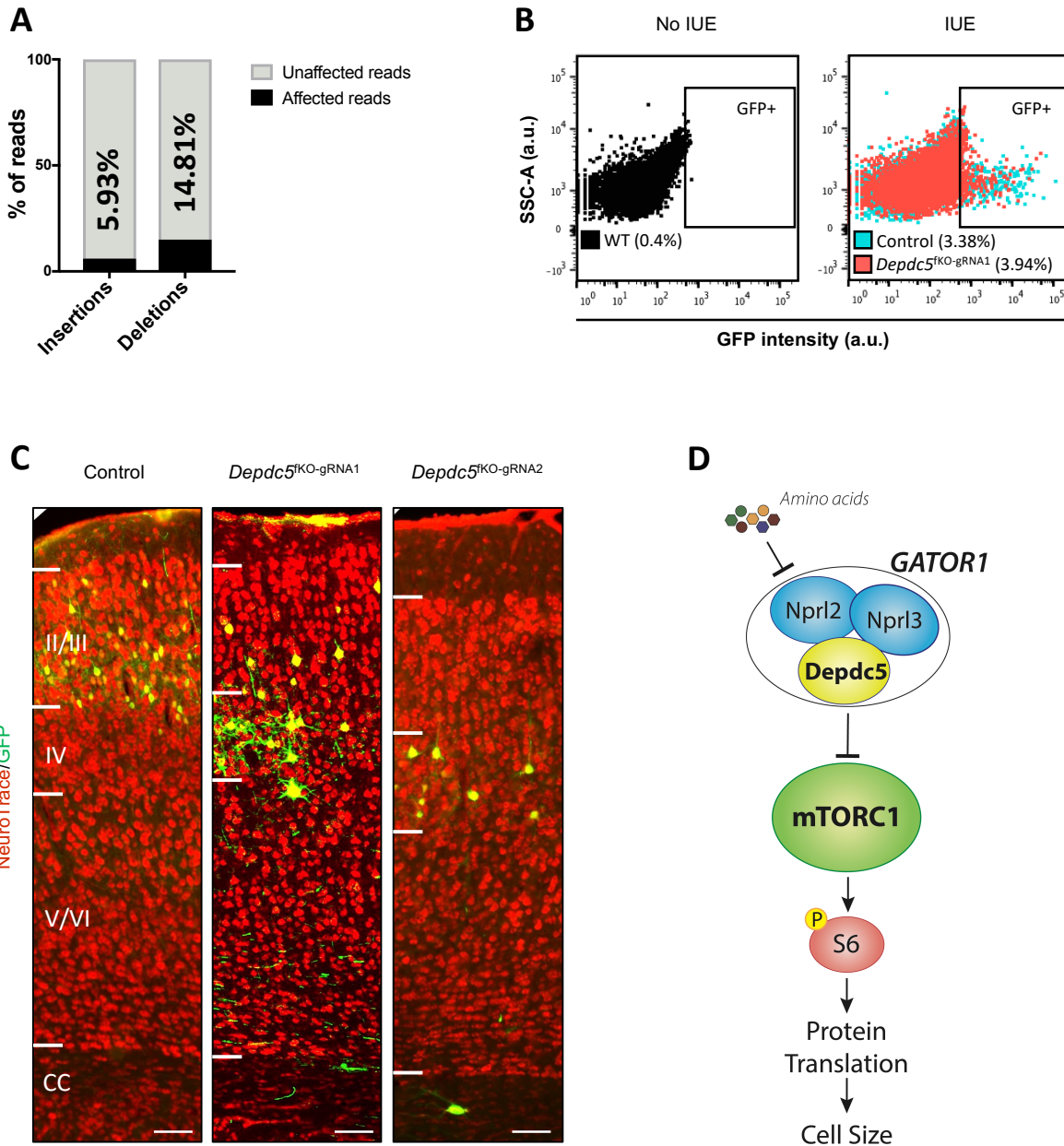
Supplemental reference

30. Mashiko D, et al. Generation of mutant mice by pronuclear injection of circular plasmid expressing Cas9 and single guided RNA. *Scientific reports*. 2013;3(3355).



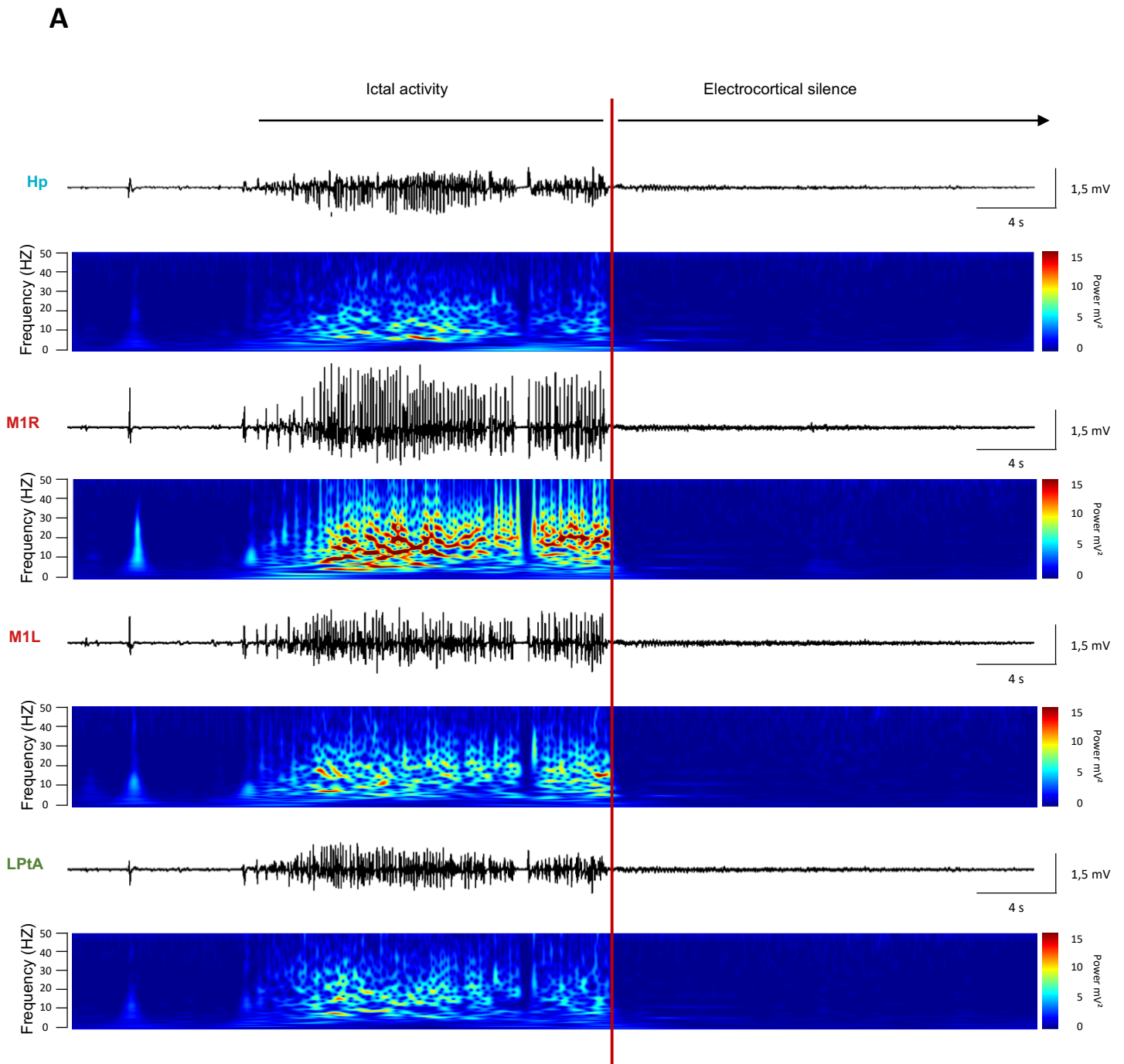
Supplementary Figure 1. Design and validation of the CRISPR-Cas9 strategy.

(A) Gene organization of mouse *Depdc5*. Targeted exon 16 is indicated. Both guide RNAs (gRNAs) 1 and 2 are indicated in green on the nucleotide sequence spanning c.1515:1535 and c.1465:1485 respectively on mm10/GRCm38 reference mouse genome, NM_001025426 transcript. Protospacer adjacent motif (PAM) sequence in red. (B) *pX330* plasmid was modified by adding a T2A-mRuby2 sequence following Cas9-NLS sequence for efficient detection of Cas9-expressing transfected cells. Purple oval, nuclear localization sequence (NLS); red circle, polyA; hU6 stands for human U6 promoter sequence. *pCAG-EGxxFP* construction was modified by cloning a PCR-amplified Cas9-target sequence for homology-directed repair (HDR) restoration of native EGFP sequence. (C) Schematic representation of *pCAG-EGxxFP* HDR-mediated recombination after CRISPR-Cas9 double-strand break (DSB). (D) mRuby2⁺ cells, GFP⁺ cells and double-positive cells after co-transfection of gRNAs 1 or 2 and *pCAG-EgxxFP* in HEK293T. Between 90% and 95% of transfected mRuby2⁺ cells are GFP⁺, indicative of the CRISPR-Cas9 efficiency. Three independent experiments were performed (n=800-1200 counted cells per experiment).



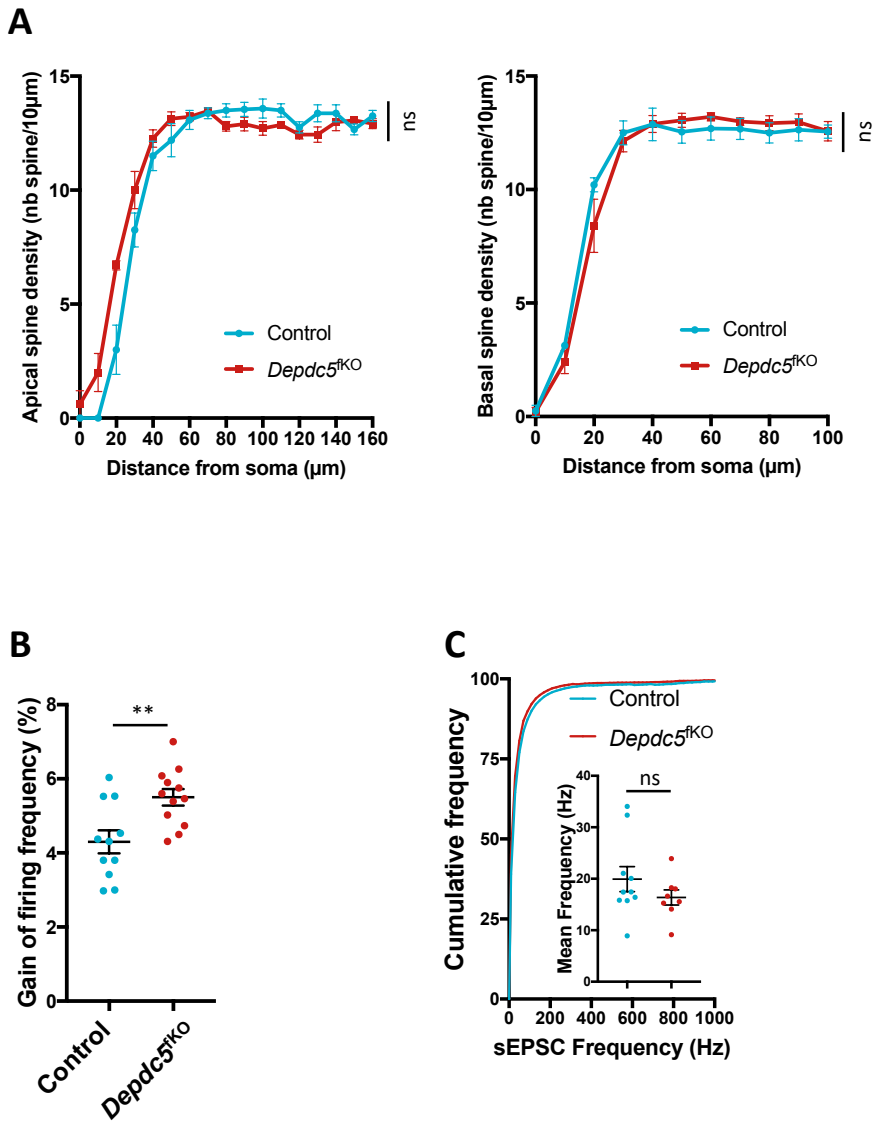
Supplementary Figure 2. CRISPR-Cas9 editing validation and histological abnormalities in *Depdc5*^{TKO} mice.

(A) Percentage of insertions and deletions (indels) in FACS-sorted GFP+ cells from *Depdc5*^{TKO-gRNA1} (53,633 indels out of 258,619 reads) and from control (74 indels out of 253,693 reads) E18.5 embryos (n=4 pooled electroporated hemispheres). **(B)** FACS-sorted GFP+ cells from electroporated, or not, hemispheres of wild-type (not electroporated), control and *Depdc5*^{TKO-gRNA1} E18.5 embryos. SSC-A, size scatter area scaling. Black squares represent gating on GFP+ cells. Numbers between parentheses indicate percentage of GFP+ cells. (n=4 non-electroporated wild-type, n=4 controls and n=4 *Depdc5*^{TKO-gRNA1}, pooled hemispheres). **(C)** Schematic representation of the amino-acid sensing GATOR1 branch of the mTORC1 pathway. **(D)** Representative coronal sections of control, *Depdc5*^{TKO-gRNA1} and *Depdc5*^{TKO-gRNA2} adult brain cortex. NeuroTrace fluorescent Nissl stain in red; GFP, green. Scale bar: 100µm.



Supplementary Figure 3. Ictal activity and SUDEP in *Depdc5*^{fKO} mice.

(A) The color-coded Fast Fourier Transform (FFT) power spectrum reveals higher amplitude and frequency changes at the cortical electrode implanted at the electroporation site on the right motor cortex (M1R). EEG recordings and FFT power spectrum of the last seizure in a *Depdc5*^{fKO-gRNA1} mouse at P54 showing a sudden electrocortical silence after the ultimate tonic-clonic seizure, and in absence of status epilepticus.



Supplementary Figure 4. Morphological and physiological characteristics of *Depdc5*^{fKO} neurons

(A) Quantification of spine density on the apical and the main basal shaft of control and *Depdc5*^{fKO-gRNA1} neurons. ^{ns}P=0.7486. (10.95 ± 0.28 spines per $10\mu\text{m}$ in control versus 10.77 ± 0.15 spines per $10\mu\text{m}$ in *Depdc5*^{fKO-gRNA1}; n=5 neurons per group, n= 2738 and 5200 spines per group; Mann-Whitney test). (B) Gain of firing frequency. **P=0.0083. (n=11 controls and n=12 *Depdc5*^{fKO-gRNA1}; Mann-Whitney test). (C) Cumulative frequency distribution and dot plots of sEPSC mean frequency. ^{ns}P=0.3154. (n=10 controls and n=8 *Depdc5*^{fKO-gRNA1}; Mann-Whitney test).

Supplemental legends

Legends of supplementary videos of seizures

Video 1. Tonic movements initiating from the left hind limb at seizure onset of the cluster of seizures reported in **Figure 4B**, indicative of a focal origin of seizure in the right hemisphere, at the electroporation site.

Video 2. Representative progression of the last seizure of a cluster in a *Depdc5*^{fKO} mouse showing a brief post-ictal tonic extension of limbs followed by muscle relaxation at the moment of death and not status epilepticus.